Available online at www.sciencedirect.com
ScienceDirect
Solid State Sciences 10 (2008) 1145–1149
www.elsevier.com/locate/ssscie

Synthesis and characterization of a new quaternary selenide $Sr_3GeSb_2Se_8$

Ching-Yi Yu [a], Ming-Fang Wang [a], Ming-Yang Chung [a], Shyue-Ming Jang [b], Jih-Chen Huang [b], Chi-Shen Lee [a,*]

[a] *Department of Applied Chemistry and Institute of Molecular Science, National Chiao Tung University, 1001 Ta-Hsueh Road, Hsinchu 30010, Taiwan*
[b] *Industrial Technology Research Institute, N300, UCL/ITRI Building 22, 321, Kuang Fu Road, Section 2, Hsinchu 300, Taiwan*

Received 1 August 2007; received in revised form 26 November 2007; accepted 10 December 2007
Available online 23 December 2007

Abstract

A new quaternary selenide $Sr_3GeSb_2Se_8$ has been synthesized at 750 °C from pure elements in a stoichiometric ratio under vacuum. The product as-synthesized is characterized by single-crystal X-ray diffraction, diffuse reflectance spectroscopy, and thermoanalysis. The title compound crystallizes in the orthorhombic space group *Pnma* with $a = 12.633(4)$ Å, $b = 4.301(1)$ Å, $c = 28.693(7)$ Å, $V = 1558.8(8)$ Å^3, $Z = 4$, $R_1/wR_2 = 0.0582/0.1221$, and GOF = 1.077. The structure of $Sr_3GeSb_2Se_8$ features a new structural type that consists of one-dimensional chains of vertex-sharing tetrahedra $^1_\infty[MSe_3]$ (M = Ge/Sb) and fused double chains of edge-shared square pyramids $^1_\infty[M_2Se_5]$, which are held together by Sr^{2+} ions. A band gap of 0.75 eV for $Sr_3GeSb_2Se_8$ was derived from its diffuse reflectance spectrum.

Keywords: Crystal structure; Germanium; Antimony; Selenium; Solid-state synthesis; Semiconductor

1. Introduction

Multinary chalcogenides exhibit varied structural types that have attracted intensive research for their prospective nonlinear optics [1], ferroelectrics [2], and thermoelectric applications [3–8]. Much attention has been devoted to the synthesis of metal chalcogenides, such as $CsBi_4Te_6$ [9] and $AgPb_mSbTe_{2+m}$ [10,11], that might produce compounds with a narrow band gap for a large figure of merit ($ZT = \sigma S^2/\kappa$, where Z = figure of merit; T = temperature; S = Seebeck coefficient; σ = electrical conductivity; κ = thermal conductivity). For the reported chalcogenides, almost all main-group metals cooperate with the elements of group 16 (S, Se, Te) and alkali, alkaline-earth metals or rare-earth elements to form multinary chalcogenides [12]. Among these compounds, only a few ternary selenides Sr–Ge–X and Sr–Sb–X (X = S, Se, Te) have been structurally characterized, such as $Sr_2Ge_2Se_5$ [13], $Sr_2Ge_2X_4$ (X = S, Se) [14,15], $Sr_3Sb_4S_9$ [16], and $Sr_6Sb_6S_{17}$ [17]. Only one multinary chalcogenide $Ba_4LaGe_3SbSe_{13}$ [18], containing Ge, Sb and Se, appears to have been reported. Our exploratory research has focused on chalcogenides of the form A_e–M_1–M_2–X (alkaline-earth element A_e; M_1 = Ge, Sn; M_2 = Sb, Bi; X = S, Se, Te) system. On extending the project to the Sr–Ge–Sb–Se system, we synthesized a new quaternary chalcogenide $Sr_3GeSb_2Se_8$ having one-dimensional chains of corner-sharing tetrahedra and fused square-pyramidal double chains. Here we report the synthesis, structure and characterization of $Sr_3GeSb_2Se_8$.

2. Experiments

2.1. Synthesis

$Sr_3GeSb_2Se_8$ was synthesized by a solid-state method. The initial reagents were strontium (Sr, 99.0%, Alfa Aesar), germanium (Ge, 99.999%, Alfa Aesar), antimony (Sb, 99.5%, Alfa Aesar), and selenium (Se, 99.999%, Alfa Aesar).

* Corresponding author. Tel.: +886 3 5131332; fax: +886 3 5723764.
E-mail address: chishen@mail.nctu.edu.tw (C.-S. Lee).

1293-2558/$ - see front matter © 2007 Elsevier Masson SAS. All rights reserved.
doi:10.1016/j.solidstatesciences.2007.12.010

In a typical reaction, these pure elements in stoichiometric proportions were mixed in an Ar-filled glove box (total mass ~0.5 g), placed in a silica tube, sealed under dynamic vacuum, and heated slowly to 750 °C within 72 h. This temperature was maintained for 3 days, followed by slow cooling to 550 °C over 7 days, and finally to about 23 °C on simply terminating the power. Initial reactions were intended to synthesize '$Sr_3Ge_2Sb_2X_9$' (X = S, Se, Te). Based on the powder X-ray diffraction experiment, the S and Te reactions yield mixtures of Sr_2GeS_4, SrS for '$Sr_3Ge_2Sb_2X_9$' and SrTe, Sb_2Te_3, Te for '$Sr_3Ge_2Sb_2Te_9$' reactions. From the '$Sr_3Ge_2Sb_2Se_9$' reaction, the products contain a dark brown product with irregularly shaped crystals. As confirmed by single-crystal diffraction, we succeeded in preparing $Sr_3GeSb_2Se_8$ in quantitative yields using the elements in a stoichiometric ratio and the same heating profile as described above. Analysis of $Sr_3Ge_2Sb_2Se_9$ crystals with energy-dispersive spectra (SEM/EDX, Hitachi H-7500 Scanning Electron Microscope) showed the presence of Sr, Ge, Sb and Se. $Sr_3GeSb_2Se_8$ is sensitive to air and moisture such that it gradually decomposes to form a red amorphous powder in air in 7 days.

2.2. Single-crystal X-ray diffraction (XRD)

A single crystal of compound $Sr_3GeSb_2Se_8$ ($0.1 \times 0.1 \times 0.1$ mm^3) was mounted on a glass fiber with epoxy glue; intensity data were collected on a diffractometer (Bruker APEX CCD equipped with graphite-monochromated Mo Kα radiation, $\lambda = 0.71073$ Å) at 25(2) °C. The distance from the crystal to the detector was 5.0 cm. Data were collected in scans 0.3° in ω within groups of 600 frames each at ϕ settings 0° and 60°. The duration of exposure was 60 s/frame. The values of 2θ varied between 3.50° and 56.58°. Diffraction signals obtained from all frames of reciprocal-space images were used to determine the unit-cell parameters. The data were integrated using the Siemens SAINT program and were corrected for Lorentz and polarization effects [19]. Absorption corrections were based on fitting a function to the empirical transmission surface as sampled by multiple equivalent measurements of numerous reflections. The structural model was obtained with the direct method and refined with full-matrix least-square refinement based on F^2 using the SHELXTL package [20].

2.3. Structure determination

A dark brown crystal of $Sr_3GeSb_2Se_8$ revealed an orthorhombic unit cell ($a = 12.633(4)$ Å, $b = 4.301(1)$ Å, $c = 28.693(7)$ Å, $V = 1558.8(8)$ Å^3) and systematic absences indicated space group *Pnma* (no. 62). Using direct methods, a structural model was built with six unique sites for metal atoms (Sr, Ge and Sb) and eight unique sites for Se atoms. The crystal structure was initially refined in a model of $Sr_3GeSb_2Se_8$ with fully occupied sites of Sr (Sr(1)–Sr(3)), Ge (M(1)), Sb (M(2), M(3)) and Se (Se(1)–Se(8)). The isotropic displacement parameters (U_{iso}) of M(1)–M(3) sites exhibited unreasonable values, which indicated that M(1)–M(3) sites had partial or mixed occupancy by Ge or Sb cations. A subsequent refinement indicated that the M(1) site is occupied 65%/35% by Ge/Sb, whereas the M(2) and M(3) sites contain 6%/94% and 24%/76% of Ge/Sb, respectively. This result yielded a charge-balanced formula $Sr_3GeSb_2Se_8$. Final structural refinements yielded R_1/wR_2 to be 0.0582/0.1221. All atomic positions were refined with anisotropic displacement parameters. Tables 1–3 summarize the crystallographic data, atomic coordinates and interatomic distances of $Sr_3GeSb_2Se_8$. Further details of the crystal-structure investigation can be obtained from the Fachinformationszentrum Karlsruhe, Eggenstein-Leopoldshafen, Germany (fax: +49 7247 808 666; e-mail: crysdata@fiz.karlsruhe.de) on quoting the depository number CSD-418942.

2.4. Characterization

X-ray powder diffraction data of the products were measured on a Bragg–Brentano-type powder diffractometer (Bruker D8 Advance, operated at 40 kV and 40 mA, Cu Kα, $\lambda = 1.5418$ Å). For phase identification, XRD data were collected in a 2θ range from 5° to 60° with a step interval of 0.02°. Diffuse reflectance measurements were performed near 25 °C with a UV–visible spectrophotometer (Jasco V-570); an integrating sphere was used to measure the diffuse reflectance spectra over the range 200–2000 nm. Samples as ground powder were pressed onto a thin glass slide holder; a $BaSO_4$ plate served as reference. Thermogravimetric analyses (TGA) were performed on a thermogravimetric analyzer (Perkin–Elmer pyres). The sample was heated to 920 °C under a constant flow of N_2. Measurements of electrical resistivity were performed with the standard four-probe method on cold pressed bars ($1 \times 1 \times 5$ mm^3). The sample was annealed at 500 °C for 6 h before the measurement. For several samples, the electrical conductivity was so poor that the electrical resistance exceeded the limit (~10^3 MΩ) of the instrument.

Table 1
Crystallographic data for $Sr_3GeSb_2Se_8$

Empirical formula	$Sr_3GeSb_2Se_8$
Refined formula	$Sr_3Ge_{0.95(5)}Sb_{2.05(5)}Se_8$
Crystal size/mm^3	$0.1 \times 0.1 \times 0.1$
Formula mass/g mol^{-1}	1210.63
Temperature/K	293(2)
Wavelength/Å	0.71073
Crystal system	Orthorhombic
Space group	*Pnma* (no. 62)
a/Å	12.633(4)
b/Å	4.301(2)
c/Å	28.683(7)
V/Å^3	1558.8(8)
Z	4
Calc. density/g cm^{-3}	5.158
Absorption coefficient/mm^{-1}	34.153
Transmission range	0.5046–1
Independent reflections	2188 [R(int) = 0.0497]
GOF on F^2	1.076
R_1/wR_2 [$I > 2\sigma(I)$]	0.0518/0.1241
$\Delta\rho$ (e/Å^3)	6.412 and −4.210

Table 2
Atomic positional coordinates, isotropic displacement parameters (10^{-3} Å^2), and site occupancies for $Sr_3GeSb_2Se_8$

Atoms	Position	x	y	z	U (eq)	Occ.
Sr(1)	4c	0.1716(1)	0.2500	0.6853(1)	19(1)	
Sr(2)	4c	0.3056(1)	0.2500	0.8433(1)	20(1)	
Sr(3)	4c	0.4699(1)	0.2500	0.5877(1)	28(1)	
M(1)	4c	0.0716(2)	0.2500	0.2178(1)	41(1)	Ge 0.65(2)
						Sb 0.35(2)
M(2)	4c	0.4547(1)	0.2500	0.0672(1)	30(1)	Ge 0.06(2)
						Sb 0.94(2)
M(3)	4c	0.2656(1)	0.2500	0.4719(1)	31(1)	Ge 0.24(2)
						Sb 0.76(2)
Se(1)	4c	0.1612(1)	0.2500	0.1429(1)	21(1)	
Se(2)	4c	0.2351(1)	0.2500	0.2622(1)	21(1)	
Se(3)	4c	0.0278(2)	0.2500	0.7787(1)	88(1)	
Se(4)	4c	0.0015(1)	0.2500	0.3441(1)	18(1)	
Se(5)	4c	0.3520(1)	0.2500	0.3881(1)	19(1)	
Se(6)	4c	0.1827(1)	0.2500	0.5755(1)	27(1)	
Se(7)	4c	0.1050(2)	0.2500	0.0052(1)	36(1)	
Se(8)	4c	0.3816(1)	0.2500	0.9492(1)	36(1)	

3. Results and discussion

3.1. Structure description

$Sr_3GeSb_2Se_8$ crystallizes in a new structural type with orthorhombic space group *Pnma*, with 14 independent positions, three for Sr, three for mixed occupancy of Sb and Ge, and eight for Se atoms. The crystal structure of $Sr_3GeSb_2Se_8$ viewed along [010] is shown in Fig. 1. The major structural feature of this compound is the presence of alternative stacks of corner-shared tetrahedra and chains of edge-shared square pyramids, which are separated by Sr^{2+} ions. The Sr atoms are connected to seven or eight selenium atoms in a polyhedron close to a monocapped (Sr(2)) or bicapped (Sr(1), Sr(3)) trigonal prism with Sr–Se distances ranging between 3.1421(17) and 3.645(3) Å. The coordination environment of Sr^{2+} atoms is common in similar chalcogenides containing the Sr^{2+} cation, such as $Sr_2Ge_2Se_4$ [14], $Sr_3Sb_4S_9$ [16], and $Sr_6Sb_6S_{17}$ [17]. The M(1)–M(3) sites form a one-dimensional structure composed of corner-sharing tetrahedral chains $^1_\infty[MSe_3]$ (M(1)) and chains of edge-sharing double square pyramids $^1_\infty[M_2Se_5]$ (M(2), M(3)), which are shown in Fig. 2. For an $^1_\infty[MSe_3]$ unit, each central metal atom forms severely distorted tetrahedral units (bond angles between 93.89(9)° and 119.26(12)°) with four M–Se bonds of length 2.429(3), 2.427(2) and 2.492(2) (×2) Å, which share corners to form an infinite chain parallel to the *b*-axis (Fig. 2a). These Se(3) atoms are shared between two MSe_4 tetrahedra. The M–Se distance is greater than for regular Ge–Se (~2.35 Å) but smaller than for Sb–Se (~2.6–2.8 Å) distances, indicating that the M(1) site has a mixed occupancy. The $^1_\infty[MSe_3]$ chain is rare in antimony chalcogenides, but similar corner-sharing $GeSe_4$ one-dimensional chains are found in A_2GeX_3 (A = Na, K, Rb, Cs; X = S, Se) [21–24]. Regarding the $^1_\infty[M_2Se_5]$ unit, the M(2) and M(3) sites form distorted square-pyramidal units with four selenium atoms that share edges to form a ribbon shape with fused square-pyramidal units parallel to the *b*-axis (Fig. 2b). The distortion of the square-pyramidal unit is caused mainly by three short and two long M–Se bonds in each polyhedron. The M(2) atoms comprise three short bonds to Se between 2.611(2) and 2.774(1) Å and two longer ones at 3.020(2) Å, whereas M(3) exhibits three short M–Se bonds at 2.642(2)–2.864(2) Å

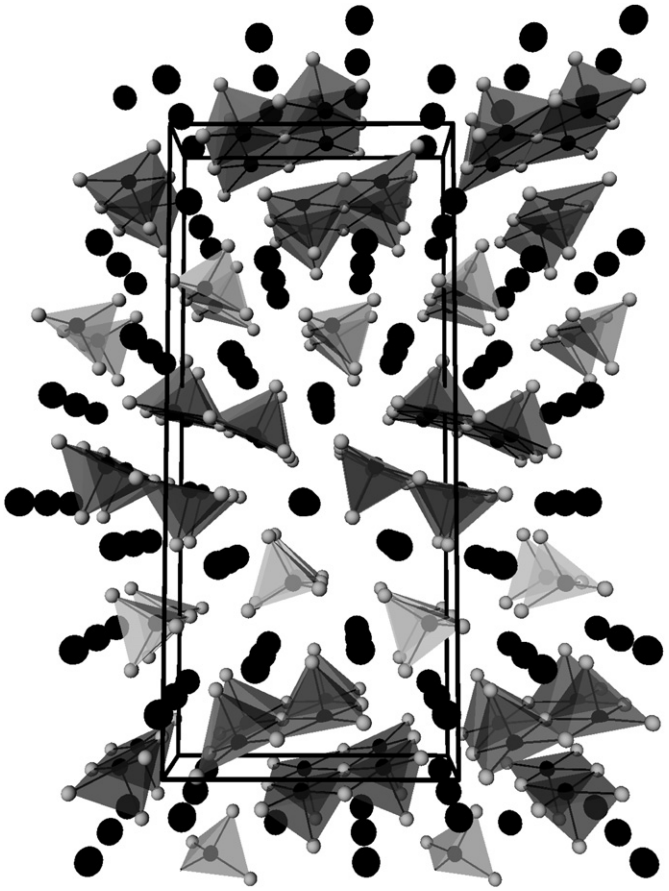

Fig. 1. (a) Polyhedral representation of $Sr_3GeSb_2Se_8$ viewed along the crystallographic *b*-axis [010], showing one-dimensional chains of $^1_\infty[MSe_3]$ (gray polyhedra) and $^1_\infty[M_2Se_5]$ (dark gray polyhedra). Big black and small gray circles denote Sr^{2+} and Se^{2-} atoms, respectively.

Table 3
Selected interatomic distances (Å) for $Sr_3GeSb_2Se_8$

Sr(1)–Se(1) × 2	3.250(2)	M(1)–Se(1)	2.429(3)
Sr(1)–Se(2) × 2	3.298(2)	M(1)–Se(2)	2.427(2)
Sr(1)–Se(3)	3.236(3)	M(1)–Se(3) × 2	2.492(2)
Sr(1)–Se(4) × 2	3.182(2)		
Sr(1)–Se(6)	3.154(2)		
		M(2)–Se(4)	2.611(2)
Sr(2)–Se(2) × 2	3.208(2)	M(2)–Se(6) × 2	2.774(1)
Sr(2)–Se(4) × 2	3.250(2)	M(2)–Se(8) × 2	3.020(2)
Sr(2)–Se(5) × 2	3.200(2)		
Sr(2)–Se(8)	3.187(2)	M(3)–Se(5)	2.642(2)
		M(3)–Se(7) × 2	2.864(2)
Sr(3)–Se(1) × 2	3.142(2)	M(3)–Se(8) × 2	2.917(2)
Sr(3)–Se(5) × 2	3.188(2)		
Sr(3)–Se(6)	3.645(3)		
Sr(3)–Se(7) × 2	3.337(2)		
Sr(3)–Se(7)	3.166(3)		

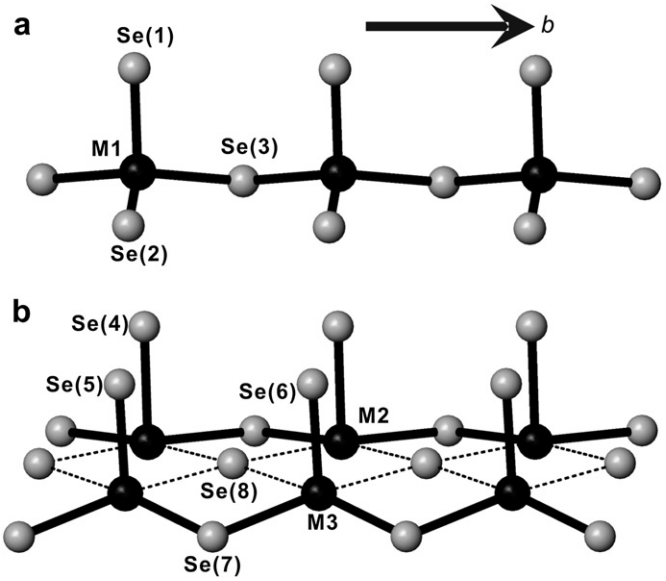

Fig. 2. (a and b) $^{1}_{\infty}[MSe_3]$ and $^{1}_{\infty}[M_2Se_5]$ chains along the [010] direction. Solid and dashed lines indicate M–Se distances <2.87 and <3.02 Å, respectively.

and two longer ones at 2.917(2) Å. The interatomic distances of M(2)-Se and M(3)-Se compare satisfactorily with the Sb–Se distances in Sb_2Se_3. The chains of fused double square pyramids form a pair that are related to each other via an *a*-glide plane parallel to the *a*-axis. Similar edge-sharing double chains were found in some multinary chalcogenides, such as $K_2Pr_{2-x}Sb_{4+x}Se_{12}$ [25] and $La_7Sb_9S_{24}$ [26]. Combining the Sr^{2+}, Ge–Se and Sb–Se anionic units, we express the charge-balanced formula as $[Sr^{2+}]_3[Ge^{4+}][Sb^{3+}]_2[Se^{2-}]_8$, which is consistent with the refined formula $Sr_3Ge_{0.95}Sb_{2.05}Se_8$.

3.2. Characterization

To determine the optical band gap, the UV–vis diffuse reflectance spectrum of ground crystals of $Sr_3GeSb_2Se_8$ was measured between 200 and 2000 nm (6.2–0.62 eV); cf. Fig. 3. $Sr_3GeSb_2Se_8$ is expected to be a semiconductor because the charge of cations and anions is balanced. Those measurements of optical diffuse reflectance reveal that the band gap is near 0.75 eV. Thermogravimetric (TGA) measurements obtained on heating polycrystalline samples reveal two stages of mass loss until the mass remains stable after 900 °C (Fig. 4). The total mass loss in these two stages drops by approximately 55%. These results were reproduced by heating the as-synthesized powder in a quartz ampoule under N_2 flow and subsequently heating to 500, 700, and 900 °C. The first decomposition step with mass loss (~5%) occurs from 400 to 500 °C (Fig. 4). X-ray powder diffraction of the material obtained at this stage showed a broad peak at $2\theta \sim 26°$ (Fig. 5). The second step starts at ~700 °C with weight loss of ~ 50%, corresponding to the decomposition of $Sr_3GeSb_2Se_8$. The PXRD pattern of the residue just before

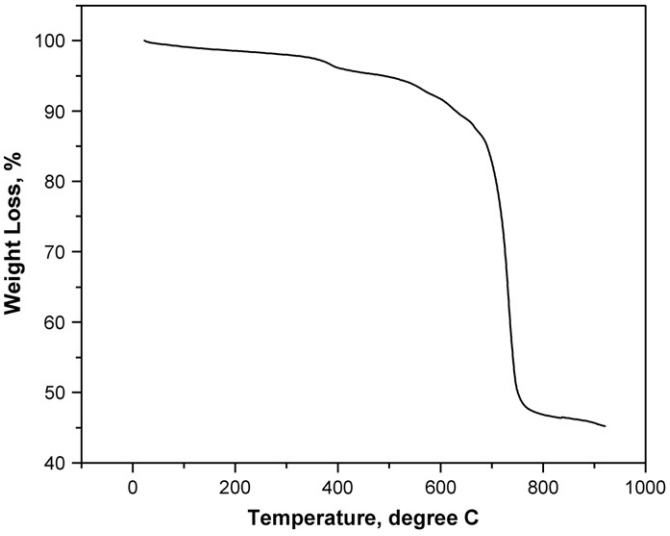

Fig. 4. Diffuse reflectance spectrum of $Sr_3GeSb_2Se_8$.

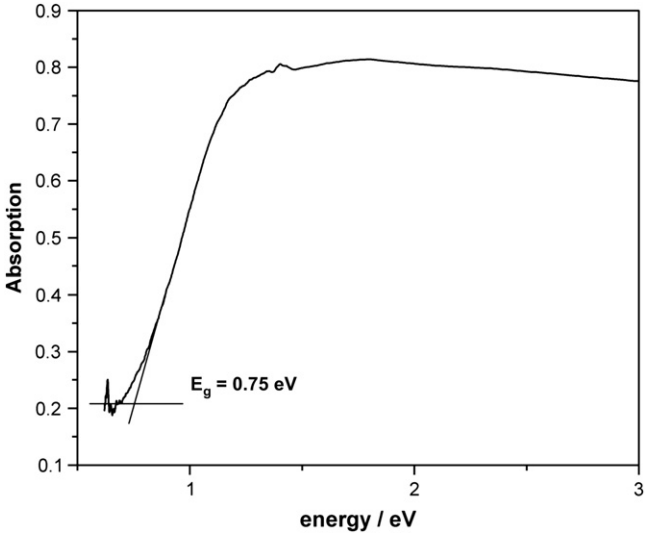

Fig. 3. TGA curve of $Sr_3GeSb_2Se_8$ (N_2 flow, heating rate = 5 °C/min).

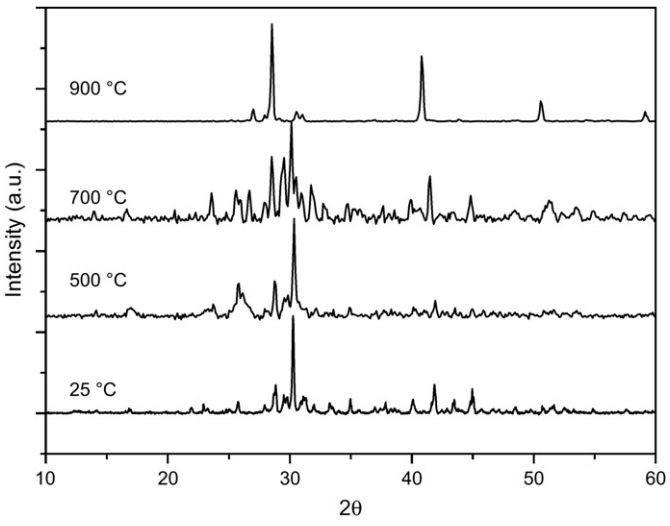

Fig. 5. Powder X-ray diffraction patterns of the residues at 25 (pure $Sr_3GeSb_2Se_8$), 500, 700, 900 °C.

the final decomposition step at 700 °C indicates that additional products of GeSe, $GeSe_2$, SrSe and the title compound are present. The PXRD pattern of the residue at 900 °C contains a mixture of crystalline SrSe and an amorphous phase. Polycrystalline product was found in the cool part of silica ampoule and the PXRD pattern can be indexed as a combination of Sb_2Se_3, GeSe, and $GeSe_2$.

4. Conclusions

We have synthesized a new quaternary selenide $Sr_3GeSb_2Se_8$ that exhibits unique one-dimensional chains of vertex-sharing tetrahedra $^1_\infty[MSe_3]$ (M = Ge/Sb) and fused double chains of edge-sharing square pyramids $^1_\infty[M_2Se_5]$. $Sr_3GeSb_2Se_8$ is an electron-precise compound with a measured band gap 0.75 eV.

Acknowledgements

We thank Prof. Eric W.G. Diau for measuring the diffuse reflectance spectrum. The National Science Council (NSC94-2113-M-009-012, 94-2120-M-009-014) supported this research.

References

[1] J.H. Liao, G.A. Marking, K.F. Hsu, Y. Matsushita, M.D. Ewbank, R. Borwick, P. Cunningham, M.J. Rosker, M.G. Kanatzidis, J. Am. Chem. Soc. 125 (2003) 9484.
[2] M. Tampier, D. Johrendt, J. Solid State Chem. 158 (2001) 343.
[3] M.G. Kanatzidis, Semicond. Semimetals 69 (2001) 51.
[4] D.M. Rowe, CRC Handbook of Thermoelectrics, CRC Press, Boca Raton, Florida, 1995.
[5] R. Venkatasubramanian, E. Siivola, T. Colpitts, B. O'Quinn, Nature 413 (2001) 597.
[6] T.M. Tritt, Thermoelectric Materials 1998 – The Next Generation Materials for Small-Scale Refrigeration and Power Generation Applications: Symposium held November 30–December 3, 1998, Boston, Massachusetts, USA, Materials Research Society, Warrendale, PA, 1999.
[7] G.S. Nolas, J. Sharp, H.J. Goldsmid, Thermoelectrics: Basic Principles and New Materials Developments, Springer, Berlin, New York, 2001.
[8] M.G. Kanatzidis, S.D. Mahanti, T.P. Hogan, Chemistry, Physics, and Materials Science of Thermoelectric Materials: Beyond Bismuth Telluride, Kluwer Academic/Plenum Publishers, New York, 2003.
[9] D.-Y. Chung, T. Hogan, P. Brazis, M. Rocci-Lane, C. Kannewurf, M. Bastea, C. Uher, M.G. Kanatzidis, Science 287 (2000) 1024.
[10] E. Quarez, K.-F. Hsu, R. Pcionek, N. Frangis, E.K. Polychroniadis, M.G. Kanatzidis, J. Am. Chem. Soc. 127 (2005) 9177.
[11] K.F. Hsu, S. Loo, F. Guo, W. Chen, J.S. Dyck, C. Uher, T. Hogan, E.K. Polychroniadis, M.G. Kanatzidis, Science 303 (2004) 818.
[12] Inorganic Crystal Structure Database, FIZ Karlsruhe and the Gmelin Institute, 2006.
[13] D. Johrendt, M. Tampier, Chem.—Eur. J. 6 (2000) 994.
[14] R. Pocha, M. Tampier, R.D. Hoffmann, B.D. Mosel, R. Poettgen, D. Johrendt, Z. Anorg. Allg. Chem. 629 (2003) 1379.
[15] E. Philippot, M. Ribes, M. Maurin, Rev. Chim. Miner. 8 (1971) 99.
[16] G. Cordier, C. Schwidetzky, H. Schaefer, Rev. Chim. Miner. 19 (1982) 179.
[17] K.S. Choi, M.G. Kanatzidis, Inorg. Chem. 39 (2000) 5655.
[18] A. Assoud, N. Soheilnia, H. Kleinke, J. Solid State Chem. 177 (2004) 2249.
[19] SAINT Version 6.22, Siemens Analytical X-ray Instruments Inc., Madison, WI, 2001.
[20] SHELXTL Version 6.10, Reference Manual, Siemens Analytical X-ray Systems, Inc., Madison, WI, 2000.
[21] J. Olivier-Fourcade, E. Philippot, M. Ribes, M. Maurin, C. R. Seances Acad. Sci., Ser. C 274 (1972) 1185.
[22] B. Eisenmann, J. Hansa, H. Schaefer, Z. Naturforsch., B: Chem. Sci. 40 (1985) 450.
[23] B. Eisenmann, J. Hansa, Z. Kristallogr. 203 (1993) 301.
[24] K.O. Klepp, F. Fabian, Z. Kristallogr. 212 (1997) 302.
[25] J.H. Chen, P.K. Dorhout, J. Alloys Compd. 249 (1997) 199.
[26] A. Assoud, K.M. Kleinke, H. Kleinke, Chem. Mater. 18 (2006) 1041.